



Boothroyd, R. J. and Warburton, J. (2020) Spatial organisation and physical characteristics of large peat blocks in an upland fluvial peatland ecosystem. *Geomorphology*, 370, 107397. (doi: [10.1016/j.geomorph.2020.107397](https://doi.org/10.1016/j.geomorph.2020.107397))

There may be differences between this version and the published version. You are advised to consult the publisher's version if you wish to cite from it.

<http://eprints.gla.ac.uk/222494/>

Deposited on 24 August 2020

Enlighten – Research publications by members of the University of Glasgow  
<http://eprints.gla.ac.uk>

1 ***Spatial organisation and physical characteristics of large peat blocks in an upland fluvial peatland***  
2 ***ecosystem***

3

4 **Authors and Affiliations**

5 Richard J. Boothroyd<sup>1,2</sup> and Jeff Warburton<sup>2</sup>

6 <sup>1</sup> School of Geographical and Earth Sciences, University of Glasgow, G12 8QQ, UK.

7 <sup>2</sup> Department of Geography, Durham University, Durham, DH1 3LE, UK.

8

9 E-mail: [richard.boothroyd@glasgow.ac.uk](mailto:richard.boothroyd@glasgow.ac.uk)

10

11 **Abstract**

12 This paper assesses the size, shape and spatial organisation of organic, carbon-rich debris (peat blocks)  
13 in an upland fluvial peatland ecosystem. Peat block inventories collected in 2002 and 2012 at an  
14 alluvial reach of Trout Beck (North Pennines; United Kingdom) provide independent surveys for  
15 investigating the physical characteristics and spatial organisation of the organic debris. Peat blocks  
16 deposited along the 450 m reach represent a substantial volume of fluvially derived in-channel  
17 sediment and carbon flux at the macroscale (total peat volume 11 m<sup>3</sup> (2002) and 17 m<sup>3</sup> (2012)). Results  
18 show that inferred peat block transport distances depend on their size and shape. Smaller and more  
19 spherical equant shaped peat blocks are transported 1.62 and 1.72 times the distance of prolate and  
20 elongate shaped peat blocks. Downstream fining relationships provide a first-order approximation of  
21 peat block degradation rates. These degradation rates are high (up to 2 mm/m for the a-axis) and  
22 indicate considerable fine sediment release during transport. Hypsometric relations show that 73%  
23 of peat blocks are distributed within 1 channel width of the thalweg, indicating lateral organisation  
24 and a pattern of preferential deposition at the active channel margin. The local effects of obstructions  
25 from topography, roughness and slope promote peat block deposition, but given the low density of  
26 the blocks and close proximity to the flow the potential for re-entrainment is high.

27

28 **Key words**

29 peat; degradation; sediment dynamics; carbon flux; abrasion; deposition

## 30 1. Introduction

31 Fluvial erosion is an important process governing the short- and long-term evolution of peatland  
32 ecosystems and can produce significant fluxes of organic carbon (Evans *et al.*, 2006). The delivery of  
33 peat from degraded peatlands provides an indicator of the erosional status and is crucial in quantifying  
34 carbon balances (Evans and Warburton, 2007). Peat transported in river channels is typically in the  
35 form of fine suspended sediment and larger, low-density ( $\sim 1050 \text{ kg m}^3$ ) peat blocks that are  
36 sometimes referred to as organic debris (Evans and Warburton, 2001; Evans and Warburton, 2007;  
37 Warburton and Evans, 2011). Peat blocks have a range of physical characteristics, often with  
38 maximum orthogonal axis dimensions on the order of centimetres to metres (Evans and Warburton,  
39 2007). They are typically classified according to their sedimentary setting and depositional form  
40 (Warburton and Evans, 2011). The implications of the processes acting on peat blocks are potentially  
41 large, given that peatlands dissected by fluvial erosion include most of the terrestrial peat store ( $\sim 3$   
42 million  $\text{km}^2$ ) and contain about 30 percent of all land-based carbon (550 GT) (IPCC, 2018). Although  
43 previous research on peat blocks has focussed on relatively steeply sloping blanket peatlands in the  
44 United Kingdom (Evans and Warburton, 2010), peat blocks are potentially widespread throughout  
45 various fluvially-dissected peatlands in different environmental settings (Figure 1); including sites of  
46 river bank failure in continuous permafrost settings (Walker *et al.*, 1987). A key aim of this paper is to  
47 demonstrate the potential rapid breakdown of peat blocks by fluvial erosion and promote awareness  
48 of this phenomena to a wider audience.

49 Fluvial sediment budgets in peatlands can become dominated by the delivery of peat from sources  
50 lateral to the channel network (Evans and Warburton, 2005; Evans *et al.*, 2006). Sediment is  
51 frequently delivered as peat blocks through cantilever bank failure of fluvially undercut blanket peat  
52 at discrete sources and more intermittently through the delivery of peat rafts via mass failure events  
53 (Dykes and Warburton, 2007). More substantial volumes of peat can be delivered to the channel  
54 network by mass failure events. Following the complex of peat slides that impacted Channerwick

55 (South Shetland; United Kingdom) on the 19<sup>th</sup> September 2003, it is estimated that ~100,000 m<sup>3</sup> of  
56 peat entered the channel network (Dykes and Warburton, 2008). A hiatus can occur between the  
57 delivery of peat blocks to the fluvial system and their subsequent entrainment and transmission (Evans  
58 and Warburton, 2001), while catchment storage processes can reduce the efficiency of sediment  
59 delivery to the downstream fluvial system and interrupt catchment export (Walling, 1983).

60 Once entrained, peat block transport depends on the critical submergence depth (block size,  $B_s$ ,  
61 relative to flow depth,  $d$ ) with three transport phases identified: flotation, saltation and rolling (Figure  
62 2) (Evans and Warburton, 2001). Transition between transport phases primarily occurs as a function  
63 of a fining peat block size or varying flow depth. During transport, the rate of degradation is linked to  
64 contact with the bed, with the rolling phase responsible for greatest losses as peat blocks split, break  
65 and abrade. Stalling/lodging can occur when the flow depth is approximately half the peat block size  
66 or less (Evans and Warburton, 2001), resulting in deposition across the active channel margin (e.g.  
67 Figure 1c). Following deposition, peat block residence times are variable and depend on whether the  
68 block is re-entrained or becomes buried in the floodplain stratigraphy. Warburton and Evans (2011)  
69 quantified an average residence time of 168 days for re-entrained blocks, compared to an average of  
70 617 days for blocks that were eventually incorporated into the floodplain stratigraphic sequence. The  
71 spatial organisation of deposited peat blocks has implications for the proportion of peat blocks that  
72 are exported out of the fluvial system, and the proportion that are locked away in the floodplain  
73 stratigraphy (Warburton and Evans, 2011).

74 Peat blocks are not usually included in carbon balance estimates of blanket peatlands dissected by  
75 fluvial erosion (Evans and Warburton, 2007). This is potentially significant because the carbon content  
76 of ombrotrophic blanket mire peat typically ranges between 50-53% dry weight (Lindsay, 2010).  
77 Fluvial carbon export primarily occurs as particulate and dissolved organic carbon (POC and DOC) and  
78 dissolved CO<sub>2</sub> (Worrall et al., 2009). POC has been shown to undergo transformation to DOC or  
79 become mineralized to CO<sub>2</sub> during periods of floodplain storage (Pawson, 2008; Pawson et al., 2012;

80 Moody et al., 2013). Evans and Warburton (2007) introduce the term 'block' organic carbon (BOC) to  
81 refer to peat blocks in organic carbon cascades, but the magnitude of flux between the carbon  
82 pathways, and the contribution and significance of peat blocks to the organic carbon cascade, remain  
83 relatively unknown. Where atmospheric interactions heighten CO<sub>2</sub> release through oxidation (Pawson  
84 *et al.*, 2012), incorporation of peat blocks into the floodplain stratigraphy allows carbon sequestration  
85 (Evans and Lindsay 2010; Warburton and Evans, 2011). Floodplains have been described as both  
86 hotspots for carbon cycling and as areas of sequestration in upland fluvial peatland ecosystems  
87 (Alderson *et al.*, 2019). An improved process-understanding of peat block transfer, degradation and  
88 residence through fluvial systems is essential for establishing representative carbon budgets (Evans  
89 and Warburton, 2007).

90 Ecologically, peat blocks represent a macroscale roughness element that impart flow heterogeneity  
91 to the channel (Crowe and Warburton, 2007). This produces a spatial patchiness in flow field dynamics  
92 and contributes towards the unequal provision of turbulence, a key abiotic factor in microhabitat  
93 provision (Davis and Barmuta, 1989). Peat blocks contribute towards the areas of channels capable  
94 to act as refugia, provide food resources and remove waste; all of which are required for the consistent  
95 functioning of invertebrate and macroinvertebrate ecosystems (Townsend, 1989; Bouckaert and  
96 Davis, 1998; Beisel *et al.*, 2000; Passy, 2001). Fine sediment is eroded from the sides of deposited peat  
97 blocks (Crowe and Warburton, 2007) where organic sediment is a key control on invertebrate  
98 ecosystem dynamics (Rice et al., 2001) and fine particulate organic sediment accumulations are  
99 associated with significant changes in macroinvertebrate biodiversity (Ramchunder et al., 2012). Short  
100 pulses of organic sediment have a negative association with the benthos and macroinvertebrate  
101 community composition (Aspray et al., 2017) and sedimentation can alter headwater invertebrate  
102 biodiversity, decreasing the density and richness at the community level (Brown et al., 2019). Fine  
103 sediment release from peat blocks has a range of ecological significances.

104 Here, we aim to improve the understanding of the physical characteristics and spatial organisation of  
105 peat blocks in an upland peatland ecosystem dissected by fluvial erosion. By constraining the quantity  
106 and distribution of peat blocks, we will contribute towards better understanding the geomorphic,  
107 carbon and ecological functioning of the peatland riverscape. This will be achieved by comparing two  
108 temporally independent peat block inventories collected in 2002 and 2012 and linking these to a high-  
109 resolution topographic dataset. The independence of the two inventories, spaced 10 years apart, can  
110 be justified based on the high turnover of peat blocks within the active fluvial system (Warburton and  
111 Evans, 2011) and the contrasting weathered form of long-term stored peat blocks cf. freshly delivered  
112 blocks. Physical characteristics (i.e. size and shape) will be related to their hypsometric distribution to  
113 better understand the spatial patterns and gradients of peat blocks across the riverscape. Results will  
114 improve our understanding of the extent and distribution of carbon-rich debris in an actively eroding  
115 peatland ecosystem, relevant for catchment sediment and carbon budgets. The paper considerably  
116 differs from previous work by Evans and Warburton (2001) that focussed on mechanisms and patterns  
117 of peat block transfer; and Warburton and Evans (2011) that concentrated on sedimentation  
118 implications around deposited blocks. The main objectives are threefold, to:

- 119 1) Produce spatially referenced inventories for peat block size and shape from repeat surveys.
- 120 2) Compare physical characteristics between temporally independent inventories, to  
121 determine the coherence and persistence of peat block characteristics.
- 122 3) Understand the spatial organisation of peat block distributions with respect to:
  - 123 i). Inferred distance downstream from discrete peat sources (for first-order  
124 approximations of peat block degradation rates and fine sediment release).
  - 125 ii). Vertical and lateral organisation relative to the channel thalweg using hypsometric  
126 relations (to assess depositional patterns and processes).

## 127 2. Materials and Methods

### 128 2.1 Study site

129 Field data were collected along a 450 m reach of an upland peatland channel in the Trout Beck  
130 catchment (11.4 km<sup>2</sup>), situated in the Moor House National Nature Reserve (North Pennines; United  
131 Kingdom) (Figure 3a). Across the catchment it is estimated that 17% of the peat blanket has been  
132 actively eroded (Garnett and Adamson, 1997), with dendritic type I gullying producing wandering  
133 channels on lower gradient slopes and linear type II gullying aligned normal to the slope on steeper  
134 gradients (Bower 1961). The peat type is dominated by *Eriophorum* sp, *Calluna vulgaris* and  
135 *Sphagnum* sp and has been accumulating for approximately 7500 years since the late Boreal (Conway,  
136 1954). Blanket peat covers ~90% of the catchment, with the depth averaging 1-3 m (Holden and Burt,  
137 2003). Blanket peat overlies the dominant surficial geology of reworked periglacial tills and fluvially  
138 derived overbank deposits (Aitkenhead *et al.*, 2002). The bedrock geology is of the Carboniferous  
139 sequence, consisting of almost horizontally interbedded limestones, sandstones and shales (Johnson  
140 and Dunham, 1963).

141 Multiple lower order surficial peatland streams combine to form the higher order Trout Beck channel,  
142 a tributary of the River Tees (Figure 3a). The channel bed is composed of poorly sorted cobble sized  
143 clasts, where the D<sub>50</sub> value ranges from 8-80 mm (Crowe and Warburton, 2007). The bedrock outcrops  
144 in the Trout Beck channel produce an alternating sequence of alluvial and bedrock reaches (Ferguson  
145 *et al.*, 2017). The selected alluvial study reach (Figure 3b) has an elevation of ~540 m, is characterised  
146 by an average slope of 0.015, and has an average wetted width of approximately 10 m. The channel  
147 is surrounded by a narrow fragmentary floodplain which in part is laterally confined by steep banks.  
148 Discharge is monitored at a downstream compound Crump weir, maintained by the Environment  
149 Agency (EA) as part of the Environmental Change Network (ID 25003). In the period of record 1957-  
150 2018 (81% completeness), mean daily flow was 0.56 m<sup>3</sup>/s, 10% exceedance (Q<sub>10</sub>) was 1.56 m<sup>3</sup>/s and  
151 5% exceedance (Q<sub>5</sub>) was 2.30 m<sup>3</sup>/s (NRFA, 2020).

152 Three discrete peat sources where cantilever failure of the blanket peat was observed were identified  
153 and mapped (Figure 3b). Peat sources were identified in the field by looking at the degree of  
154 undercutting, steepness of banks, presence of failed peat blocks and disturbance of vegetation (Evans  
155 and Warburton, 2005). The study site represents an actively eroding alluvial reach of Trout Beck, so  
156 peat block release is likely to be higher than in nearby semi-alluvial and bedrock reaches, where the  
157 potential for bank erosion is reduced. However, similar actively eroding alluvial reaches are observed  
158 further upstream and in neighbouring catchments (e.g. River Tees), so the study site is representative  
159 of the wider behaviour of the upland fluvially-dissected peatland ecosystem.

160

## 161 *2.2 Peat block inventories*

162 We collected field data on multiple site visits in October 2012. The contemporary inventory was  
163 spatially referenced using a Garmin eTrex H GPS unit, mapping the location of peat blocks, peat  
164 sources and the channel thalweg with a typical horizontal accuracy of < 1 m. For each of the mapped  
165 peat blocks, three orthogonal axis length measurements were recorded (a-, b- and c-axis;  $\pm 0.01$  m  
166 error). Only peat blocks with an a-axis length greater than 0.1 m were sampled ( $n = 127$ ). A  
167 comparable inventory, using identical survey methods, was collected along the same study reach in  
168 February 2002 ( $n = 123$ ); except a Magellan GPS ProMARK X CP was used for spatial referencing. The  
169 decadal interval between repeat surveys allows for the general governing physical processes to be  
170 tested. A first-order approximation of peat block volume was made by assuming a cubic shape and  
171 multiplying orthogonal axis lengths (a-axis \* b-axis \* c-axis). Peat block shape was classified by plotting  
172 the ratio of b-axis/a-axis against c-axis/b-axis to produce a Zingg-type diagram, with shape classified  
173 as elongate, equant, prolate or tabular. Classifying peat blocks using orthogonal axis dimensions has  
174 the additional benefit of relating directly to the characteristic mechanics of block transport (e.g.  
175 rolling, saltating, etc) (Evans and Warburton, 2001). Peat block morphology is represented by the  
176 Corey shape index (sphericity, 0-1) and disk-rod index (disk-rodness, 0-1) (Sneed and Folk, 1958;

177 Illenberger, 1991). From the nearby gauging station, peak daily flow for the 12 months preceding the  
178 2002 inventory was 4.88 m<sup>3</sup>/s (event occurred 18 days before the inventory; annual record 77%  
179 complete) and 11.7 m<sup>3</sup>/s in 2012 (event occurred 115 days before the inventory; annual record 100%  
180 complete).

181

### 182 *2.3 Digital Elevation Model (DEM)*

183 A Leica Geosystems Real Time Kinetic differential GPS 1200 (RTK dGPS) was used to survey channel  
184 and floodplain topography in April 2012. Elevation measurements were recorded at 28671 discrete  
185 points and interpolated to produce a digital elevation model (DEM) with a spatial resolution of 0.5 m.  
186 The DEM was used for the topographic analysis of the peat block inventory, with the area of DEM data  
187 coverage shown in Figure 3b.

188

### 189 *2.4 Inferred transport distances and the spatial organisation of deposited peat blocks*

190 We used the mapped peat block positions and the DEM to undertake spatial and topographic analyses.  
191 We inferred peat block transport distances by measuring the Euclidean distance from the upstream  
192 edge of peat sources to individual peat blocks. Transport was assumed to initiate from the nearest  
193 peat source, with transport only possible in the downstream direction. Rationale for this assumption  
194 is based on the presence of semi-alluvial and bedrock reaches immediately upstream of the study  
195 reach (Ferguson *et al.*, 2017). For peat blocks transported through the semi-alluvial and bedrock  
196 reaches, mechanical breakdown is assumed to be high from channel bed and sidewall contact along a  
197 0.3 km long bedrock gorge with topographic irregularities that have a sidewall roughness length on  
198 the order of several decimetres (Ferguson *et al.*, 2019). In addition, the size and morphology of the  
199 peat blocks, stored in a given reach, is often diagnostic of locally-sourced versus far-travelled blocks

200 i.e. far-travelled peat blocks are much smaller and have far greater rounding than locally-sourced  
201 material.

202 Furthermore, we quantified the vertical and lateral organisation of peat blocks relative to the mapped  
203 channel thalweg. Hypsometric relations were investigated by plotting peat block frequency and  
204 volume against: (i) vertical height above; and (ii) lateral distance away from the channel thalweg. The  
205 channel thalweg provides a temporally consistent reference point from which vertical and lateral  
206 distances were calculated. The spatial organisation of peat blocks relative to (i) and (ii) were  
207 normalised between values of 0 and 1 to compare vertical and lateral peat block distributions. These  
208 data provide hypsometric relations, allowing for the identification of zones where peat block  
209 distribution is relatively abundant or sparse.

## 210 **3. Results**

### 211 *3.1 Spatial distribution of peat blocks*

212 Peat blocks are deposited in several clusters in the 2012 inventory (Figure 4). This tendency for  
213 clustering was previously demonstrated across a range of environmental settings (Figure 1) and  
214 suggests that it is unusual for peat blocks to be deposited in isolation. Peat blocks tend not to be  
215 deposited within the active region of the channel, instead deposition is favoured at the margins of the  
216 channel on mid-channel bars, or overbank on floodplain pockets proximal to channel bends. Similar  
217 spatial distributions are repeated in other reaches in the catchment. Furthermore, peat blocks are  
218 rarely located close to the sources of cantilever bank failure. For the few peat blocks that do appear  
219 immediately downstream (< 10 m) from source zones (3% in 2002; 2% in 2012), it is assumed that  
220 these peat blocks have recently failed and are yet to be entrained by high flows. This indicates  
221 dispersion of peat blocks, supporting the argument for peat blocks being efficiently transferred  
222 through the fluvial system (Evans and Warburton, 2001).

223

### 224 *3.2 Peat block size and classified shape*

225 There is considerable variation in the size of peat blocks in the 2002 and 2012 inventories (Figure 5;  
226 Table 1). A range of values are recorded across peat block orthogonal axes, with the range in a-axis  
227 exceeding 2 m and the range in b-axis exceeding 1 m. Standard deviations are equivalent to  
228 approximately 50% of the mean axis lengths, indicating substantial variation in orthogonal axis  
229 dimensions. Peat block dimensions vary and this is temporally consistent between the inventories  
230 (Figure 5). The data on orthogonal axes are non-normally distributed; positive skewness values,  
231 particularly for a-axis and volume, indicate there are few extremely large values. The positive kurtosis  
232 values, particularly for volume, indicate the data are heavily tailed (Figure 5). Due to the marked  
233 variation in peat block size, it is difficult to generalise peat block dimensions to a characteristic value.

234 Instead, peat block dimensions are reported to be on the order of centimetres to metres. Comparing  
235 the total estimated volume of peat blocks, the inventory from 2012 (16.68 m<sup>3</sup>) is 58.9% larger than  
236 the inventory in 2002 (10.50 m<sup>3</sup>). This represents a considerable volume of both sediment and carbon  
237 flux at the macroscale.

238 In terms of shape, the mean a-axis typically exceeds the mean b-axis by approximately 1.5-2,  
239 suggesting that characteristic peat block shape is non-cubic. Peat block shape is classified by plotting  
240 the ratio of b-axis/a-axis against c-axis/b-axis to produce a Zingg-type diagram (Figure 6). Elongate  
241 shapes are most abundant in the 2002 inventory (46%), followed by prolate (27%), tabular (22%) and  
242 equant (5%). In the 2012 inventory, equant shapes are most abundant (42%), followed by tabular  
243 (22%), prolate (20%) and elongate (16%). The sparsity of equant peat blocks in the 2002 inventory is  
244 notable and demonstrates that the proportions of classified shapes has changed through time,  
245 indicating temporal incoherence in classified shape.

246 The relationships between peat block size (b-axis and volume) and classified shape are shown in Figure  
247 7 and Table 2. For equant, elongate and prolate shaped peat blocks, the differences in b-axis and  
248 volume are not statistically significant between the 2002 and 2012 inventories (Mann-Whitney test,  
249  $p$ -value > 0.001). For tabular shaped peat blocks, the differences in b-axis and volume are statistically  
250 significant between 2002 and 2012 (Mann-Whitney test,  $p$ -value < 0.001). When classified by shape,  
251 the size of most peat blocks has remained the same through time, indicating temporal coherence in  
252 peat block size. Where the 2002 and 2012 inventories are combined, differences in b-axis and volume  
253 are not statistically significant between peat blocks of different classified shape (Kruskal Wallis test,  
254 b-axis:  $p$ -value > 0.001; volume:  $p$ -value > 0.001). Overall, peat blocks with different classified shapes  
255 are not significantly different in size.

256

257 *3.3 Inferred peat block transport distances*

258 The mean inferred transport distance has almost doubled from 64.07 m in 2002 to 120.79 m in 2012  
259 (Table 1). Peat block transport distances are greater in the 2012 inventory and this difference is  
260 statistically significant (Mann-Whitney test,  $p$ -value  $< 0.001$ ). A summary of the changes in peat block  
261 size, morphology and inferred transport distance for the classified shapes are shown in Table 2.  
262 Statistically significant differences in the inferred transport distance between peat blocks of different  
263 classified shape are noted (Kruskal Wallis test,  $p$ -value  $< 0.001$ ). Equant shaped blocks are transported  
264 the greatest mean distance (125.60 m), have the smallest peat block size and were most spherical  
265 (mean Corey shape index of 0.73). Evans and Warburton (2007) had previously suggested a positive  
266 feedback whereby smaller peat blocks are transported greater distances. Tabular shaped blocks are  
267 transported a mean distance of 101.78 m, have a comparably small mean volume ( $0.08 \text{ m}^3$ ), but  
268 differed from equant shaped blocks in terms of a lower sphericity and more disk-like morphology  
269 (mean disk-rod index of 0.32). Shorter mean transport distances are shown for prolate (77.59 m) and  
270 elongate (73.23 m) shaped blocks. Prolate shaped blocks have a larger mean block volume ( $0.18 \text{ m}^3$ )  
271 and more rod-like morphology (mean disk-rod index 0.84); whereas elongate shaped blocks have the  
272 lowest overall block sphericity (mean Corey shape index of 0.36). Therefore, equant shaped peat  
273 blocks are transported 1.62 and 1.72 times the distance of prolate and elongate shaped peat blocks,  
274 and this difference is statistically significant (Mann-Whitney tests,  $p$ -value  $< 0.001$ ).

275

### 276 *3.4 First-order approximations of peat block degradation rates*

277 Downstream fining relationships are shown in Figure 8, with considerable scatter an artefact of the  
278 clustering and spatial organisation of deposited peat blocks (e.g. 150-200 m downstream). Inferred  
279 peat block transport distances for the 2002, 2012 and combined inventories are regressed against  
280 orthogonal axes (Figure 8a-c). First-order approximations of peat block degradation rates are  
281 estimated by fitting a linear regression to block axes and the inferred transport distance. The  
282 statistical relationship between a-axis and transport distance is characterised by a low coefficient of

283 determination ( $R^2 = 0.097$ ), but a statistically significant negative slope ( $\alpha = -0.00245$  and  $p$ -value <  
284 0.001). The slope of the regression corresponds to an a-axis degradation rate of 2.45 mm/m ( $n = 250$ ).  
285 Caution is noted when using this approach; the low coefficient of determination indicates that only a  
286 small fraction of the variance is explained by the parameters, and there is considerable scatter in  
287 downstream fining sequences. Regressions for the b-axis and c-axis are not presented because the  
288 coefficient of determinations were lower, and the slopes not statistically significant. By applying the  
289 same process to a sample of b-axis peat block measurements collected at Trout Beck in 1997 published  
290 in Evans and Warburton (2007), a similar order of magnitude in peat block degradation rate is  
291 quantified (4.18 mm/m;  $n = 61$ ). Although these estimates provide only a first-order approximation  
292 of peat block degradation rates, they indicate the rapid breakdown of transported peat blocks;  
293 consistent with measurements of specific abrasion rates from field experiments on small peat blocks  
294 (Evans and Warburton, 2001).

295 Peat block degradation rates are used to estimate fine sediment release (Table 3). From the inferred  
296 transport distance of each peat block, a characteristic range of peat block degradation rates are  
297 applied to back-calculate initial peat block volumes (i.e. pre-transport) and estimate the potential  
298 volume of fine sediment release. Degradation rate scenarios are designed to represent the first-order  
299 degradation rates quantified here, and illustrate both equal (a-axis = b-axis = c-axis) and unequal (a-  
300 axis > b-axis > c-axis) degradation losses across peat block orthogonal axes. Were the peat block  
301 degradation rates an order of magnitude lower than those estimated here (i.e. DR1, 0.5 mm/m a-, b-  
302 and c-axis), 1.66 m<sup>3</sup> of fine sediment would have been released in the 2002 inventory and 5.34 m<sup>3</sup> in  
303 the 2012 inventory. This fine sediment release would represent 14 and 24% of the pre-transport peat  
304 block volume. Were the peat block degradation rates comparable to those estimated here (i.e. DR3,  
305 2 mm/m a-, b- and c-axis), substantially greater volumes of fine sediment would have been released  
306 (2002 = 9.64 m<sup>3</sup> or 48% of the pre-transport peat block volume; 2012 = 32.08 m<sup>3</sup> or 66% of pre-  
307 transport peat block volume). Were peat block losses only recorded across the a-axis (i.e. DR5, 2  
308 mm/m a-axis, no losses b- and c-axis), then volumes of fine sediment release are smaller (2002 = 0.96

309 m<sup>3</sup> or 8% of the pre-transport peat block volume; 2012 = 3.86 m<sup>3</sup> or 19% of pre-transport peat block  
310 volume). Finally, if peat block degradation rates were comparable to those estimated here, but  
311 unequal across orthogonal axes (i.e. DR6, 2 mm/m a-axis, 1 mm/m b-axis and 0.5 mm/m c-axis), then  
312 considerable volumes of fine sediment would be released (2002 = 3.39 m<sup>3</sup> or 24% of the pre-transport  
313 peat block volume; 2012 = 11.99 m<sup>3</sup> or 42% of the pre-transport peat block volume). Scenario testing  
314 reveals the potentially large volumes of fine sediment released from inventoried peat blocks during  
315 transport (mean average of DR1-DR7 estimates in 2002 = 8.35 m<sup>3</sup>; 2012 = 28.54 m<sup>3</sup>).

316

### 317 *3.5 Spatial organisation of deposited peat blocks*

318 To better understand the spatial organisation of deposited peat blocks from the 2012 inventory,  
319 normalised vertical heights and lateral distances from the channel thalweg are mapped (Figure 9) and  
320 the abundance quantitatively assessed using hypsometric relations (Figure 10). All mapped peat  
321 blocks lie within a tight vertical height range from the channel thalweg (0-0.71 m); whereas the range  
322 of lateral distances is wider (0-21.08 m). For hypsometric relations, divergence from  $x = y$  indicates  
323 either an abundance (flatter sections) or sparseness (steeper sections) of deposited peat blocks.

324 The vertical organisation (Figure 9a) shows that spatial clusters of peat blocks have similar normalised  
325 heights above the channel thalweg (e.g. the group of peat blocks perched on the mid-channel bar are  
326 associated with similar heights above the channel thalweg). Hypsometric relations (Figure 10a) show  
327 that peat blocks are almost uniformly distributed with height above the channel thalweg, with only  
328 minor deviations from the line of equality. The associated histogram shows that 28% of peat blocks  
329 are distributed in the lower third of the normalised profile, 44% in the middle third, and 28% in the  
330 upper third. This suggests that peat block deposition is almost equally likely over the range of mapped  
331 heights. The tight range of heights and uniform vertical distribution above the channel thalweg  
332 suggest that peat blocks are transported close to the maximum stage of flood flows. Peat block

333 deposition through stalling is sensitive to the small changes in the hydraulic surface (Figure 2), and  
334 this sensitivity is recorded in the spatial organisation of deposited peat blocks.

335 The lateral organisation of peat blocks (Figure 9b) demonstrates preferential deposition proximal to  
336 the channel thalweg. Peat block transport is therefore aligned to the channel thalweg. Hypsometric  
337 relations (Figure 10b) show a more marked deviation from the line of equality, with an abundance of  
338 peat blocks at normalised lateral distances in the range 0.2-0.5. The zone where relatively more peat  
339 blocks are deposited extends approximately 1 channel width (up to ~10.5 m) from the channel  
340 thalweg. The associated histogram shows that 73% of peat blocks are distributed within 1 channel  
341 width of the thalweg, and that many of the largest peat blocks by volume are deposited here. A  
342 relatively sparse zone is shown at normalised distances > 0.75 (towards 2 channel widths from the  
343 channel thalweg), so fewer peat blocks are deposited beyond the active channel margin. The  
344 pronounced lateral organisation, with preferential deposition proximal to the active channel margin,  
345 suggest that peat blocks tend to be transported close to the channel thalweg (i.e. approximately within  
346 the confines of the active channel) and that deposition is associated with local obstructions from  
347 topography, roughness and changes in slope at the active channel margin.

348 For each peat block, normalised vertical and lateral positions are shown in Figure 11. For peat blocks  
349 deposited in or around the active channel margin, the normalised height above the thalweg increases  
350 with normalised distance from the channel thalweg, with most of the volumetrically largest peat  
351 blocks deposited in this zone. The relationship is indicative of rapid deposition associated with small  
352 changes in hydraulic surface. Beyond the active channel margin relatively few peat blocks are  
353 deposited over a smaller range of heights. The hypsometric relations observed at Trout Beck suggest  
354 an underlying spatial organisation on peat block deposition; transport is aligned to the channel  
355 thalweg and small changes in the hydraulic surface and/or local obstructions from topography,  
356 roughness and slope promote peat block deposition at the active channel margin.

357

358 **4. Discussion**

359 Through the analysis of two temporally independent inventories collected in 2002 and 2012, peat  
360 blocks are characterised as having principal axes on the order of centimetres to metres, showing  
361 variation in their size and shape. Locally, individual peat blocks can represent large depositional  
362 features (maximum measured a-axis: 3.05 m; maximum estimated volume: 1.59 m<sup>3</sup>). Large peat  
363 blocks have geomorphological and ecological significance, locally modifying the flow, controlling the  
364 deposition of gravel and even influencing channel planform (Evans and Warburton, 2007). The  
365 proportion of classified peat block shapes has changed through time; elongate shaped peat blocks  
366 were most abundant in 2002, whereas equant shaped peat blocks were most abundant in 2012 (Figure  
367 6). Between classified peat block shapes, no statistically significant difference in peat block size was  
368 observed. Although most classified peat block shapes remained approximately the same size between  
369 inventories (Figure 7); only tabular shaped blocks showed a statistically significant difference in b-axis  
370 and volume. Results from Trout Beck suggest a temporal consistency in peat block size.

371 We suggest that the natural variation in peat block size and shape is influenced by three key factors:  
372 (i) the block delivery mechanism that imparts a control on the initial, unmodified peat block; (ii) the  
373 flow history that acts to modify peat blocks during in-channel processing; and (iii) the residence time  
374 of the peat block in the channel environment between transport events. Cantilever failure of peat  
375 banks is identified to be the principal delivery mechanism for peat blocks at Trout Beck (Evans and  
376 Warburton, 2001). This will provide initial peat blocks with highly variable physical characteristics,  
377 analogous to the complex assemblages of basal slump blocks in alluvial channels (Hackney *et al.*,  
378 2015). The material properties of the source material will exert a control on peat block shape, with  
379 peat blocks sourced from the fibrous upper layer of the blanket peatland likely to have a more tabular  
380 shape, whereas peat blocks sourced from the basal lower peat likely have a more equant shape.  
381 Following entrainment, in-channel processing will rework and modify the physical characteristics of  
382 peat blocks, with mechanical breakdown through splitting, breakage and abrasion (Figure 2).

383 Experimental work has suggested that a critical submergence depth equivalent to peat block depth is  
384 required to initiate peat block movement (Warburton and Evans, 2001). The potential for  
385 entrainment, and consequently the extent of reworking and modification, will therefore depend on  
386 the hydraulic surface and flow velocity. Flow conditions in the lead up to the temporally independent  
387 inventories differed, with the peak daily flow in the 12 months preceding the 2012 inventory more  
388 than double that of the 2002 inventory (2002 = 4.88 m<sup>3</sup>/s; 2012 = 11.7 m<sup>3</sup>/s). Hence, the temporal  
389 sequencing of flow events would impart a control on the physical characteristics observed. Finally,  
390 significant hiatuses between peat block delivery, eventual entrainment/re-entrainment and  
391 deposition could result in further modifications of peat blocks. Recently delivered or deposited peat  
392 blocks that remain stationary but immersed in water for extended time periods have material  
393 removed during geomorphologically effective flow events (Wood *et al.*, 2001), so flow exposure may  
394 modify the physical characteristics. In addition, peat blocks will be exposed to progressive breakdown  
395 and weathering through wetting and drying, freeze-thaw, ice-needle growth and rainfall events which  
396 may significantly alter their physical characteristics and surface texture (Evans and Warburton 2001;  
397 Evans and Warburton, 2007; Li *et al.*, 2018). These three factors likely influence the physical  
398 characteristics of peat blocks observed in upland fluvial peatland ecosystems.

399 Following the link discontinuity concept (Rice and Church, 1998), mapped peat sources provide  
400 significant lateral input of peat blocks, with channel reaches between the inputs acting as sedimentary  
401 links. However, downstream fining over the study reach is disrupted by internal hydraulic peat block  
402 sorting sequences associated with preferential deposition on mid-channel bars and clustering on the  
403 floodplain (Figure 4, 8 and 9). Analogous to downstream fining in gravel-bed rivers, considerable noise  
404 can be introduced by complex sedimentary features that build up during numerous flow events of  
405 various magnitude, with different sizes of material supplied from upstream (Hoey and Bluck, 1999).  
406 This disruption explains the observed variation in downstream fining over the sedimentary links (e.g.  
407 at 150-200 m downstream in Figure 8) and is inherent to the longitudinal distribution of peat blocks  
408 in upland fluvial peatland ecosystems.

409 Hypsometric relations show an underlying spatial organisation of peat blocks across the study reach  
410 with small changes in the hydraulic surface and/or local obstructions from topography, roughness and  
411 slope promoting rapid peat block deposition proximal to the active channel margin. The tight range  
412 of heights and uniform vertical distribution above the channel thalweg record the sensitivity to  
413 changes in hydraulic surface and support rapid deposition by stalling (Figure 2). Flow diversion and  
414 localised reductions of flow velocity have been associated with the deposition of peat blocks (Newall  
415 and Hughes, 1995; Evans and Warburton, 2001). In-channel and floodplain roughness elements may  
416 enhance the likelihood of deposition, as evidenced by the clustering of peat blocks on mid-channel  
417 bars (Figure 4). Interactions between floodplain vegetation (e.g. sedge patches) and flow could cause  
418 localised velocity reductions, heightening the potential for peat block deposition at the active channel  
419 margin (Evans and Warburton, 2001). Lateral heterogeneities in roughness elements surrounding the  
420 active channel contribute to the spatial organisation of peat blocks at Trout Beck, influencing peat  
421 block transport efficiency and their potential fate (i.e. potential for incorporation into the floodplain  
422 stratigraphic sequence).

423 Photo archive evidence from the lower section of the Trout Beck study reach showed that 74% of  
424 deposited peat blocks in the period 1997-2008 were re-entrained back into the flow, rather than  
425 buried into the floodplain stratigraphic sequence (Warburton and Evans, 2011). Hypsometric relations  
426 show that peat blocks are deposited proximal to the active channel margin, where the re-entrainment  
427 potential is high. Once entrained, the rates of peat block degradation are high (particularly through  
428 abrasion), so peat blocks can constitute a significant source of fine sediment release (Evans and  
429 Warburton, 2007). With the volume of peat blocks periodically renewed by bank and bluff erosion,  
430 peat blocks represent a dynamic component of the fluvially derived sediment and organic matter  
431 budget (Evans and Warburton, 2001; Crowe and Warburton, 2007).

432 Our inventories show that peat blocks represent a significant volume of fluvially derived in-channel  
433 sediment at the macroscale (11 m<sup>3</sup> in 2002 and 17 m<sup>3</sup> in 2012). The first-order approximations of peat

434 block degradation rates indicate considerable fine sediment release during transport; while photo  
435 archive imagery and hypsometric relations at this site suggest that floodplain burial is unlikely. In  
436 compiling a sediment budget for the nearby Rough Sike catchment (0.83 km<sup>2</sup>, North Pennines; United  
437 Kingdom), Evans and Warburton (2005) showed a net sediment input of 8 m<sup>3</sup> was delivered annually  
438 as peat blocks from an actively failing peat bank (33 m in length). At the catchment scale, the volume  
439 of bank erosion at Rough Sike (and therefore fine sediment release) was budgeted to be 28.5 m<sup>3</sup> a<sup>-1</sup>.  
440 For the larger Trout Beck catchment (11.4 km<sup>2</sup>), we estimate that comparable volumes of fine  
441 sediment are released from the transport and in-channel processing of peat blocks along a single  
442 actively eroding alluvial reach (e.g. DR3 in 2012, Table 3). Peat blocks are not only morphologically  
443 important but also represent an important source of fine sediment in peatland ecosystems. Although  
444 this sediment flux is widely recognised, the contribution of peat blocks to catchment sediment budgets  
445 represent a significant knowledge gap (Evans and Burt, 2010).

446 With high peat block transport efficiencies, peat blocks can rapidly degrade and release organic  
447 material (Crowe and Warburton, 2007). Given the low potential for storage in channel beds, this  
448 organic material is exported from the catchment so represents a significant loss of terrestrial carbon  
449 (Crowe and Warburton, 2007). Carbon sequestration can take place if peat blocks are eventually  
450 incorporated into the sedimentary sequence (Evans and Lindsay 2010; Warburton and Evans, 2011),  
451 but results from the Trout Beck study reach suggest this is unlikely. Crucially, carbon budget studies  
452 are increasingly used by upland managers to inform and implement land strategies on carbon  
453 stewardship, with the fluvial component the second largest contributor to the upland terrestrial  
454 carbon budget (Warburton and Evans 2011). Omission of the fluvial component could lead to a  
455 significant underestimation of the total carbon flux (Webster and Meyer, 1997), and here we advocate  
456 for recognition of the BOC component within such budgets. Further field and flume experimentation  
457 are needed for the quantification of peat block entrainment thresholds, transport phases and detailed  
458 degradation losses (both fine sediment and organic carbon). The implications for large peat blocks in  
459 catchment sediment budgets and organic carbon cascades are particularly relevant given that blanket

460 peatlands have experienced severe erosion and will experience an increasing erosion risk from 21<sup>st</sup>  
461 century climate change (Evans and Warburton, 2007; Li *et al.*, 2016; Li *et al.*, 2017); raised awareness  
462 and improved process-understanding for this phenomena is therefore vital.

## 463 5. Conclusions

464 This paper has investigated the physical characteristics (size and shape) and spatial organisation of  
465 peat blocks in an upland peatland dissected by fluvial erosion. Through collection of two temporally  
466 independent peat block inventories, first-order approximations of peat block degradation rates and  
467 estimates of fine sediment release have been provided. Key findings include:

- 468 1. Peat blocks are variable in size, with orthogonal axis dimensions on the order of centimetres  
469 to meters. Peat block a-axes typically exceed the b-axes by 1.5-2 and a range of peat block  
470 shapes are classified. The proportion of classified peat block shapes varies between the  
471 temporally independent inventories (e.g. equant shaped blocks represent 5% of the total in  
472 2002, 42% in 2012), but the size (b-axis and volume) remains temporally coherent.
- 473 2. Peat blocks represent a substantial volume of fluviially derived sediment and carbon flux at  
474 the macroscale. The total volume of measured peat blocks was 10.50 m<sup>3</sup> in 2002, this  
475 increased by 59% to 16.68 m<sup>3</sup> in 2012.
- 476 3. Inferred peat block transport distances support a positive feedback with smaller and more  
477 spherical peat blocks are transported greater distances (Evans and Warburton, 2007). Equant  
478 shaped blocks are transported the greatest distances (125.60 m), have the smallest  
479 characteristic size and have the most spherical morphology. Shorter average transport  
480 distances are shown for prolate (77.59 m) and elongate (73.23 m) shaped blocks. Prolate  
481 shaped blocks have a larger average block volume and more rod-like morphology; whereas  
482 elongate shaped blocks have the lowest sphericity. In addition to a size-control, the shape  
483 and morphology of peat blocks influence transmission through fluvial systems.
- 484 4. Downstream fining relationships provide a first-order approximation for peat block  
485 degradation rates, these are high (up to 2 mm/m for the a-axis) and indicate considerable fine  
486 sediment release during peat block transport (e.g. DR3: 9.64 m<sup>3</sup> in 2002; 32.08 m<sup>3</sup> in 2012).

- 487 5. Hypsometric relations show a spatial organisation of peat blocks across the study reach. 73%  
488 of peat blocks are distributed within 1 channel width of the channel thalweg, indicative of  
489 preferential deposition proximal to the active channel margin.
- 490 6. Future work is needed to improve the process-understanding of peat block of transmission  
491 and in-channel processing. This includes field and flume experimentation for the  
492 quantification of peat block entrainment thresholds, transport phases and detailed  
493 degradation losses (sediment and organic carbon). This is necessary to better constrain  
494 catchment sediment budgets and organic carbon cascades in actively eroding, fluvially-  
495 dissected upland peatland ecosystems.

496 **Acknowledgments**

497 We would like to thank Natural England and UK Centre for Ecology & Hydrology ECN Central  
498 Coordination Unit for access to the Moor House National Nature Reserve and co-operation. Work  
499 related to this project was partly funded by a NERC (NE/F010141/1) award to JW. We are grateful to  
500 Mark Kinsey and Sarah Crowe for access to unpublished data. We would like to thank Rich Hardy for  
501 helpful comments on an earlier version of this manuscript. The authors are grateful to the Editor and  
502 two anonymous reviewers for providing helpful comments that led to significant improvements in this  
503 manuscript.

504

505 **Data availability**

506 Data used in this manuscript can be obtained by contacting the lead author.

507 **References**

- 508 Aitkenhead, N., Barclay, W.J., Brandon, A., Chadwick, R.A., Chisholm, J.I., Cooper, A.H., Johnson,  
509 E.W., 2002. British Regional Geology: The Pennines and Adjacent Areas. British Geological Society,  
510 Nottingham.
- 511
- 512 Alderson, D.M., Evans, M.G., Rothwell, J.J., Rhodes, E.J., Boulton, S., 2019. Geomorphological controls  
513 on fluvial carbon storage in headwater peatlands. *Earth Surface Processes and Landforms*. 44(9), pp.  
514 1675-1693.
- 515
- 516 Aspray, K.L., Holden, J., Ledger, M.E., Mainstone, C.P., Brown, L.E., 2017. Organic sediment pulses  
517 impact rivers across multiple levels of ecological organization. *Ecohydrology*. 10(6), e1855.
- 518
- 519 Beisel, J-N., Usseglio-Polatera, P., Moreteau, J-C., 2000. The spatial heterogeneity of a river bottom:  
520 a key factor determining macroinvertebrate communities. *Hydrobiologia*. 422-423, pp. 163-171.
- 521
- 522 Bouckaert, F.W., Davis, J., 1998. Microflow regimes and the distribution of macroinvertebrates  
523 around stream boulders. *Freshwater Biology*. 40(1), pp. 77-86.
- 524
- 525 Bower, M.M., 1961. The Distribution of Erosion in Blanket Peat Bogs in the Pennines. *Transactions  
526 and Papers (Institute of British Geographers)*. 29, pp. 17-30.
- 527
- 528 Brown, L.E., Aspray, K.L., Ledger, M.E., Mainstone, C.P., Palmer, S.M., Wilkes, M., Holden, J., 2019.  
529 Sediment deposition from eroding peatlands alters headwater invertebrate biodiversity. *Global  
530 Change Biology*. 25(2), pp. 602-619.
- 531
- 532 Conway, V.M., 1954. Stratigraphy and Pollen Analysis of Southern Pennine Blanket Peats. *Journal of  
533 Ecology*. 42(1), pp. 117-147.
- 534
- 535 Crowe, S., Warburton, J., 2007. Significance of large peat blocks for river channel habitat and stream  
536 organic budgets. *Mires and Peat*. 2, pp. 1-15.
- 537
- 538 Davis, J.A., Barmuta, L.A., 1989. An ecologically useful classification of mean and near-bed flows in  
539 streams and rivers. *Freshwater Biology*. 21(2), pp. 271-282.
- 540

541 Dykes, A.P., Warburton, J., 2007. Mass movements in peat: A formal classification scheme.  
542 *Geomorphology*. 86(1-2), pp. 73-93.  
543

544 Dykes, A.P., Warburton, J., 2008. Characteristics of the Shetland Islands (UK) peat slides of 19  
545 September 2003. *Landslides*. 5(2), pp. 213-226.  
546

547 Evans, M., Burt, T.P., 2010. Erosional Processes and Sediment Transport in Upland Mires, in: Burt, T.,  
548 Allison, R., (eds), *Sediment Cascades: An Integrated Approach*. Wiley, Hoboken, pp. 217-240.  
549

550 Evans, M., Lindsay, J., 2010. High resolution quantification of gully erosion in upland peatlands at the  
551 landscape scale. *Earth Surface Processes and Landforms*. 35(8), pp. 876-886.  
552

553 Evans, M., Warburton, J., 2001. Transport and dispersal of organic debris (peat blocks) in upland  
554 fluvial systems. *Earth Surface Processes and Landforms*. 26(10), pp. 1087-1102.  
555

556 Evans, M., Warburton, J., 2005. Sediment budget for an eroding peat-moorland catchment in  
557 northern England. *Earth Surface Processes and Landforms*. 30(5), pp. 557-577.  
558

559 Evans, M., Warburton, J., 2007. *The geomorphology of upland peat: erosion, form and landscape*.  
560 Blackwell, Oxford.  
561

562 Evans, M., Warburton, J., Yang, J., 2006. Eroding blanket peat catchments: Global and local  
563 implications of upland organic sediment budgets. *Geomorphology*. 79(1-2), pp. 45-57.  
564

565 Evans, M., Warburton, J., 2010. *Peatland Geomorphology and Carbon Cycling*. *Geography Compass*.  
566 4(10), pp. 1513-1531.  
567

568 Ferguson, R.I., Sharma, B.P., Hardy, R.J., Hodge, R.A., Warburton, J., 2017. Flow resistance and  
569 hydraulic geometry in contrasting reaches of a bedrock channel. *Water Resources Research*. 53(3),  
570 pp. 2278-2293.  
571

572 Ferguson, R.I., Hardy, R.J., Hodge, R.A., 2019. Flow resistance and hydraulic geometry in bedrock  
573 rivers with multiple roughness length scales. *Earth Surface Processes and Landforms*, 44(12),  
574 pp.2437-2449.

575

576 Garnett, M.H., Adamson, J.K., 1997. Blanket mire monitoring and research at Moor House Nature  
577 Reserve. Macaulay Land Use Research Institute, Aberdeen.

578

579 Garnett, M., Adamson, J.K., 1997. Blanket mire monitoring and research at Moor House National  
580 Nature Reserve, in: Tallis, J.H., Meade, R., Hulme, P.D., (eds), Blanket Mire Degradation: Causes and  
581 Consequences. British Ecological Society, Aberdeen, pp. 116-117.

582

583 Hackney, C., Best, J., Leyland, J., Darby, S.E., Parsons, D., Aalto, R., 2015. Modulation of outer bank  
584 erosion by slump blocks: Disentangling the protective and destructive role of failed material on the  
585 three-dimensional flow structure. *Geophysical Research Letters*. 42, pp. 10663-10670.

586

587 Hoey, T.B., Bluck, B.J., 1999. Identifying the controls over downstream fining of river gravels. *Journal*  
588 *of Sedimentary Research*. 69(1), pp. 40-50.

589

590 Holden, J., Burt, T.P., 2003. Runoff production in blanket peat covered catchments. *Water Resources*  
591 *Research*. 39(7), 1191.

592

593 Johnson, G.A.L., Dunham, K.C., 1963. The geology of Moor House. Monographs of the Nature  
594 Conservancy Council Number Two. HMSO, London.

595

596 Illenberger, W.K., 1991. Pebble shape (and size!). *Journal of Sedimentary Research*. 61(5), pp. 756-  
597 767.

598

599 IPCC., 2018: Global warming of 1.5°C. An IPCC Special Report on the impacts of global warming of  
600 1.5°C above pre-industrial levels and related global greenhouse gas emission pathways, in the  
601 context of strengthening the global response to the threat of climate change, sustainable  
602 development, and efforts to eradicate poverty. Available at: <http://ipcc.ch/report/sr15/> (accessed 20  
603 March 2020).

604

605 Labadz, J.C., Burt, T.P., Potter, A.W.R., 1991. Sediment yield and delivery in the blanket peat  
606 moorlands of the southern Pennines. *Earth Surface Processes and Landforms*. 16(3), pp. 255-271.

607

608 Li, P., Holden, J., Irvine, B., 2016. Prediction of blanket peat erosion across Great Britain under  
609 environmental change. *Climate Change*. 134(1-2), pp. 177-191.

610

611 Li, P., Holden, J., Irvine, B., Mu, X., 2017. Erosion of Northern Hemisphere blanket peatlands under  
612 21st-century climate change. *Geophysical Research Letters*. 44(8), pp. 3615-3623.

613

614 Li, C., Holden, J., Grayson, R., 2018. Effects of needle ice on peat erosion processes during overland  
615 flow events. *Journal of Geophysical Research: Earth Surface*. 123(9), pp. 2107-2122.

616

617 Lindsay, R., 2010. Peatbogs and carbon: a critical synthesis to inform policy development in oceanic  
618 peat bog conservation and restoration in the context of climate change. Environmental Research  
619 Group, University of East London.

620

621 Moody, C.S., Worrall, F., Evans, C.D., Jones, T., 2013. The rate of loss of dissolved organic carbon  
622 (DOC) through a catchment. *Journal of Hydrology*. 492, pp. 139-150.

623

624 Newall, A.M., Hughes, J.M.R., 1995. Microflow environments of aquatic plants in flowing water  
625 wetlands, in: Hughes, J.M.R., Heathwaite, A.L., (eds). *Hydrology and Hydrochemistry of British*  
626 *Wetlands*. Wiley, Chichester, pp. 363-381.

627

628 National River Flow Archive (NRFA). 2020. 25003 - Trout Beck at Moor House. Accessed July 2020:  
629 <https://nrfa.ceh.ac.uk/data/station/meanflow/25003>

630

631 Passy, S.I., 2001. Spatial paradigms of lotic diatom distribution: a landscape ecology perspective.  
632 *Journal of Phycology*. 37(3), pp. 370-378.

633

634 Pawson, R.R., 2008. Assessing the role of particulates in the fluvial organic carbon flux from eroding  
635 peatland systems. PhD thesis, University of Manchester.

636

637 Pawson, R.R., Lord, D.R., Evans, M., Allott, T.E.H., 2008. Fluvial organic carbon flux from an eroding  
638 peatland catchment, southern Pennines, UK. *Hydrology and Earth System Science*. 12(2), pp. 625-  
639 634.

640

641 Pawson, R.R., Evans, M., Allott, T.E.H., 2012. Fluvial carbon flux from headwater peatland streams:  
642 significance of particulate carbon flux. *Earth Surface Processes and Landforms*. 37(11), pp. 1203-  
643 1212.

644

645 Planet Team., 2017. Planet Application Program Interface: In Space for Life on Earth. San Francisco,  
646 CA. <https://api.planet.com>.

647

648 Ramchunder, S. J., Brown, L. E., Holden, J., 2012. Catchment-scale peatland restoration benefits  
649 stream ecosystem biodiversity. *Journal of Applied Ecology*. 49, pp. 182-191.

650

651 Rice, S.P., Church, M., 1998. Grain size along two gravel-bed rivers: statistical variation, spatial  
652 pattern and sedimentary links. *Earth Surface Processes and Landforms*. 23(4), pp. 345-363.

653

654 Rice, S.P., Greenwood, M.T., Joyce, C.B., 2001. Tributaries, sediment sources, and the longitudinal  
655 organisation of macroinvertebrate fauna along river systems. *Canadian Journal of Fisheries and*  
656 *Aquatic Sciences*. 58(4), pp. 824-840.

657

658 Sneed, E.D., Folk, R.L., 1958. Pebbles in the lower Colorado River, Texas a study in Particle  
659 Morphogenesis. *Journal of Geology*. 66(2), pp. 114-150.

660

661 Townsend, C.R., 1989. The Patch Dynamics Concept of Stream Community Ecology. *Journal of the*  
662 *North American Benthological Society*. 8(1), pp. 36-50.

663

664 Walling, D.E., 1983. The sediment delivery problem. *Journal of Hydrology*. 65(1-3), pp. 209-237.

665

666 Walker, J., Lennart, A., Peippo, J., 1987. Riverbank Erosion in the Colville Delta, Alaska. *Geografiska*  
667 *Annaler*. 69(1), pp. 711–720.

668

669 Warburton, J., Evans, M., 2011. Geomorphic, sedimentary, and potential palaeoenvironmental  
670 significance of peat blocks in alluvial river systems. *Geomorphology*. 130(3-4), pp. 101-114.

671

672 Webster, J.R., Meyer, J.L., 1997. Stream Organic Matter Budgets: An Introduction. *Journal of the*  
673 *North American Benthological Society*. 16(1), pp. 3-13.

674

675 Worrall, F., Burt, T.P., Rowson, J.G., Warburton, J., Adamson, J.K., 2009. The multi-annual carbon  
676 budget of a peat-covered catchment. *Science of The Total Environment*. 407(13), pp. 4084-4094.  
677

## Tables

**Table 1** – Summary statistics of peat block size and inferred transport distances for the 2002, 2012 and combined inventories.

Inventory	Dimension	Mean	Median	Range	Standard deviation	Skewness	Kurtosis	Number of blocks
2002	<i>a-axis (m)</i>	0.69	0.52	2.93	0.54	2.39	9.43	123
	<i>b-axis (m)</i>	0.32	0.28	0.97	0.17	0.96	4.35	
	<i>c-axis (m)</i>	0.18	0.15	0.51	0.11	0.79	3.05	
	<i>Volume (m<sup>3</sup>)</i>	0.09	0.02	1.07	0.17	3.75	19.01	
	<i>Inferred transport distance (m)</i>	64.07	60.00	340.00	47.77	1.73	8.17	
2012	<i>a-axis (m)</i>	0.64	0.59	2.12	0.37	1.49	6.15	127
	<i>b-axis (m)</i>	0.42	0.41	1.08	0.20	1.08	4.34	
	<i>c-axis (m)</i>	0.28	0.25	0.73	0.13	1.26	5.22	
	<i>Volume (m<sup>3</sup>)</i>	0.13	0.06	1.59	0.24	4.21	23.11	
	<i>Inferred transport distance (m)</i>	120.79	111.84	193.97	55.46	-0.27	-1.07	
Combined	<i>a-axis (m)</i>	0.66	0.55	2.93	0.46	2.31	10.21	250
	<i>b-axis (m)</i>	0.37	0.34	1.13	0.19	1.06	4.54	
	<i>c-axis (m)</i>	0.23	0.21	0.80	0.13	1.03	4.72	
	<i>Volume (m<sup>3</sup>)</i>	0.11	0.04	1.59	0.21	4.32	25.48	
	<i>Inferred transport distance (m)</i>	92.88	93.21	340.73	59.01	0.49	0.08	

**Table 2** – Peat block size (b-axis and volume), morphology (Corey shape index and disk-rod index) and inferred distance from peat source for the classified peat block shapes in the 2002, 2012 and combined inventories.

Inventory	Peat block shape	Count	b-axis (m)		Volume (m <sup>3</sup> )		Corey shape index (-)		Disk-rod index (-)		Inferred transport distance (m)	
			Mean	Standard deviation	Mean	Standard deviation	Mean	Standard deviation	Mean	Standard deviation	Mean	Standard deviation
2002	<i>Elongate</i>	57	0.31	0.17	0.07	0.12	0.34	0.09	0.70	0.11	62.63	40.18
	<i>Equant</i>	6	0.36	0.13	0.06	0.05	0.65	0.03	0.55	0.13	44.17	25.18
	<i>Prolate</i>	33	0.30	0.18	0.14	0.26	0.49	0.10	0.86	0.09	48.03	40.46
	<i>Tabular</i>	27	0.36	0.18	0.05	0.09	0.38	0.13	0.38	0.16	91.11	62.55
2012	<i>Elongate</i>	21	0.45	0.15	0.13	0.20	0.40	0.07	0.62	0.07	102.00	62.18
	<i>Equant</i>	53	0.34	0.19	0.09	0.22	0.74	0.09	0.60	0.22	134.82	54.99
	<i>Prolate</i>	25	0.45	0.21	0.24	0.36	0.60	0.08	0.83	0.08	116.61	48.52
	<i>Tabular</i>	28	0.53	0.19	0.12	0.10	0.45	0.10	0.35	0.15	112.06	53.08
Combined	<i>Elongate</i>	78	0.35	0.18	0.09	0.15	0.36	0.08	0.68	0.11	73.23	49.87
	<i>Equant</i>	59	0.34	0.19	0.08	0.21	0.73	0.09	0.60	0.21	125.60	59.41
	<i>Prolate</i>	58	0.37	0.21	0.18	0.31	0.54	0.11	0.84	0.08	77.59	55.54
	<i>Tabular</i>	55	0.45	0.20	0.08	0.10	0.42	0.12	0.32	0.15	101.78	58.34

**Table 3** – Estimated fine sediment release under peat block degradation rate scenarios for the 2002, 2012 and combined inventories.

Inventory	Degradation rate scenario	a-axis degradation rate (mm/m)	b-axis degradation rate (mm/m)	c-axis degradation rate (mm/m)	Estimated pre-transport volume of peat blocks, (m <sup>3</sup> )	Estimated volume of fine sediment released (m <sup>3</sup> )	% of pre-transport volume released as fine sediment
2002	Surveyed	-	-	-	10.50	-	-
	DR1	0.5	0.5	0.5	12.16	1.66	13.67
	DR2	1	1	1	14.27	3.77	26.41
	DR3	2	2	2	20.14	9.64	47.86
	DR4	4	4	4	40.79	30.29	74.26
	DR5	2	0	0	11.46	0.96	8.37
	DR6	2	1	0.5	13.89	3.39	24.41
	DR7	4	2	1	19.24	8.74	45.42
2012	Surveyed	-	-	-	16.68	-	-
	DR1	0.5	0.5	0.5	22.02	5.34	24.25
	DR2	1	1	1	28.96	12.29	42.42
	DR3	2	2	2	48.76	32.08	65.8
	DR4	4	4	4	119.49	102.81	86.04
	DR5	2	0	0	20.54	3.86	18.79
	DR6	2	1	0.5	28.66	11.99	41.81
	DR7	4	2	1	48.09	31.41	65.32
Combined	Surveyed	-	-	-	27.18	-	-
	DR1	0.5	0.5	0.5	34.18	7.00	20.48
	DR2	1	1	1	43.23	16.05	37.14
	DR3	2	2	2	68.9	41.72	60.56
	DR4	4	4	4	160.28	133.1	83.04
	DR5	2	0	0	32.00	4.82	15.06
	DR6	2	1	0.5	42.55	15.38	36.13
	DR7	4	2	1	67.33	40.15	59.64

## Figures



**Figure 1** – Examples of peat blocks from a range of environmental settings, including: (a) source bank failures (Trout Beck, North Pennines, UK); (b) source peat landslide (Dooncarton, Western Ireland); (c) spatial organisation across an active channel margin (Trout Beck, North Pennines, UK); (d) weathering and erosion in-situ (Upper Tees, North Pennines, UK); (e) abraded elongate ‘spindle-form’ peat block (Trout Beck, North Pennines, UK); and (f) elongate peat block form (Severn Estuary, UK).

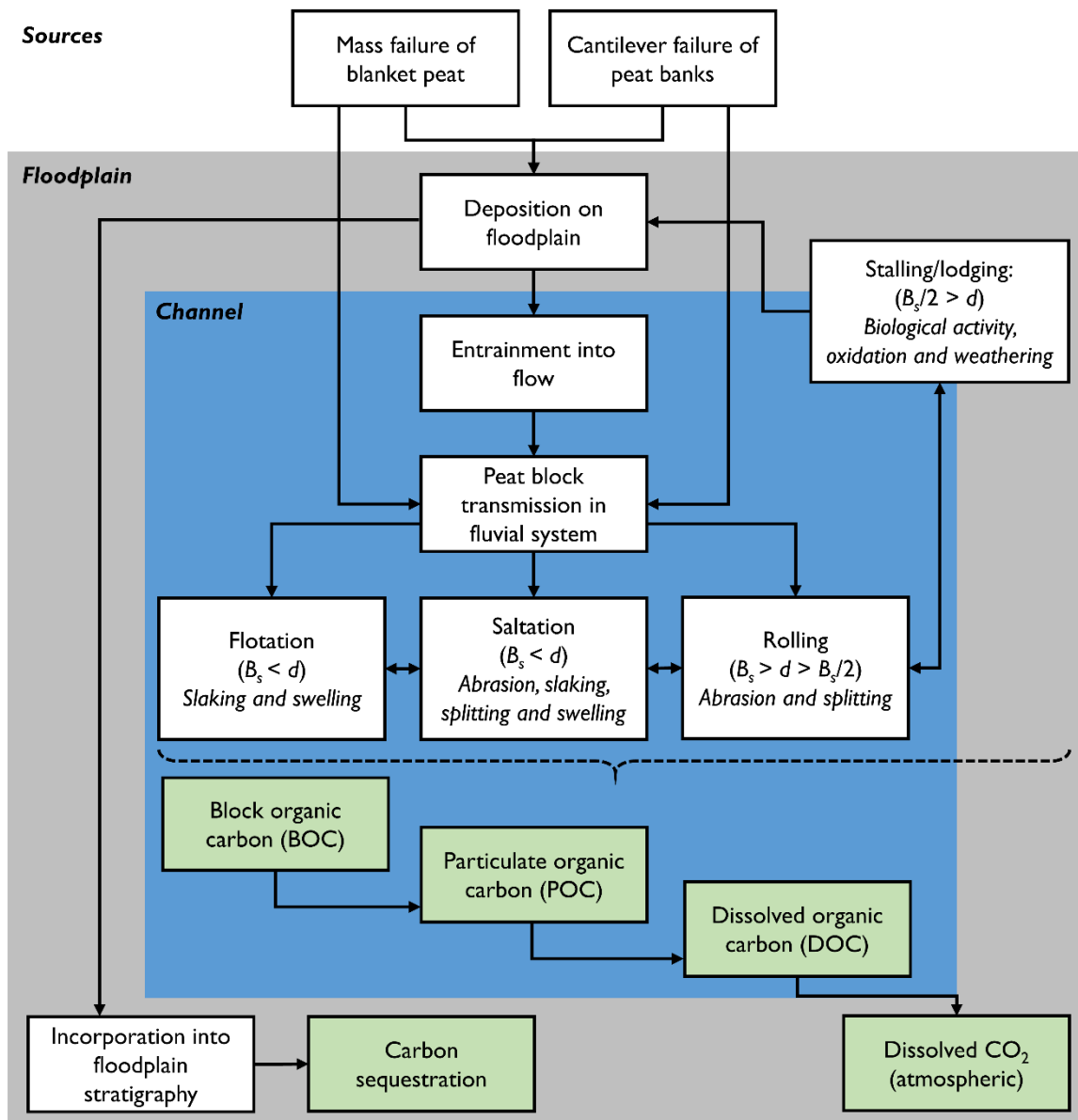


**Figure 2** – Conceptual diagram showing the delivery, in-channel processing and organic carbon cascade of peat blocks through the fluvial system. Note distinction between channel (blue) and floodplain (grey) processes and organic carbon cascade (green).  $B_s$  refers to peat block size and  $d$  refers to flow depth (modified from Evans and Warburton, 2001).

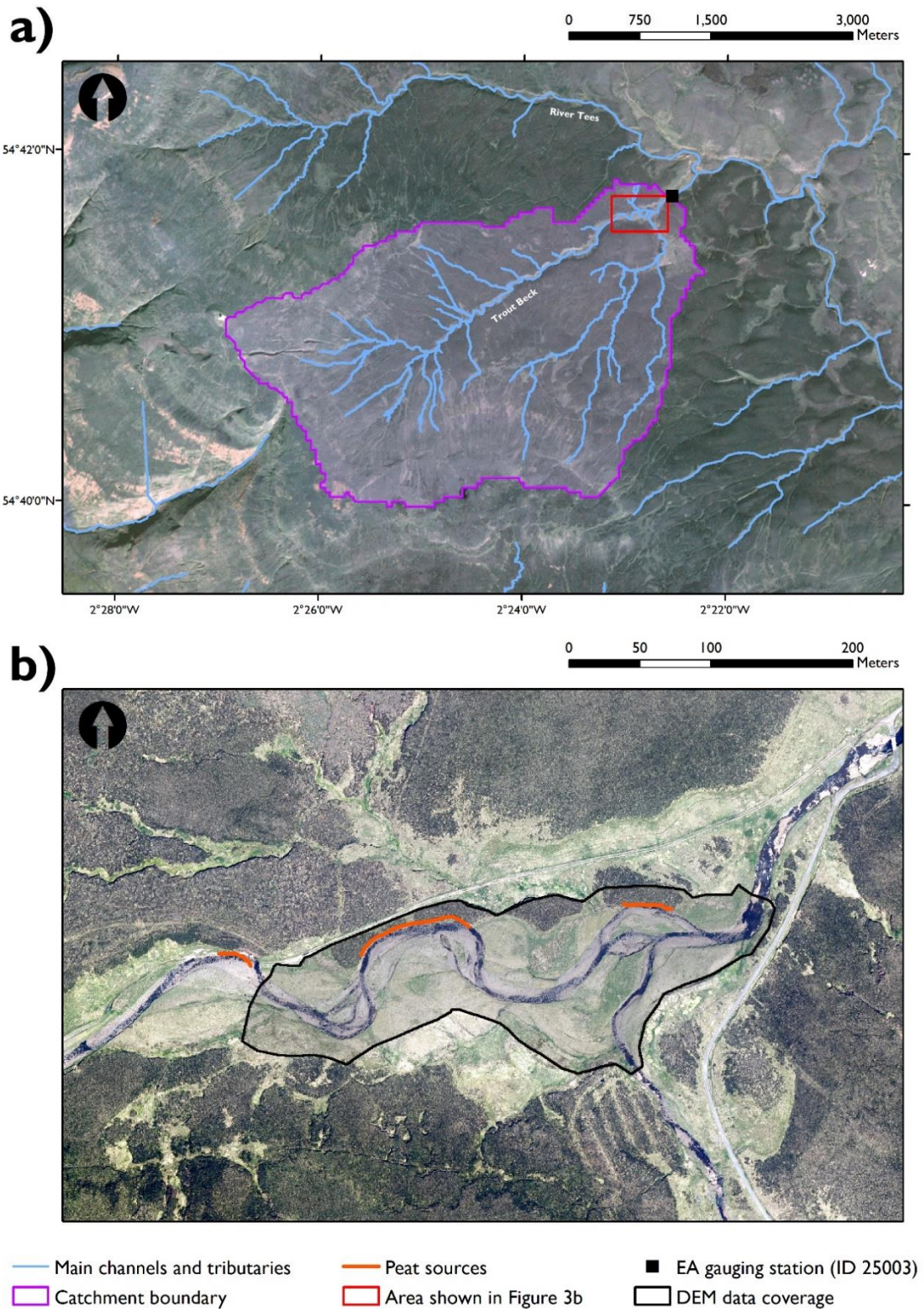


**Figure 3** – Study site overview showing: (a) the Trout Beck catchment and the Environment Agency (EA) gauging station; and (b) the study reach. Data for the catchment boundary is from National River Flow Archive (NRFA, 2020), 3 m resolution PlanetScope satellite imagery acquired 10 October 2018 (Planet Team, 2017) and 2018 aerial imagery from Edina Digimap © Getmapping Plc.

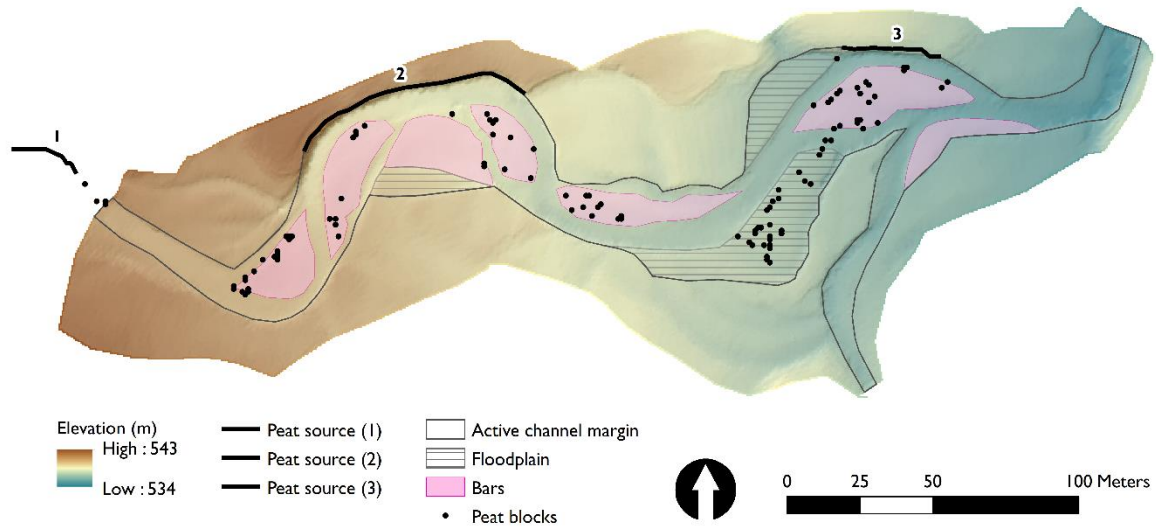


**Figure 4** – Spatial distribution of peat blocks in the 2012 inventory ( $n = 127$ ) overlaid on the hillshaded digital elevation model (DEM). Trout Beck flows from west to east. Identified peat sources are mapped and labelled (thick black lines) with several clusters of deposited peat blocks shown.

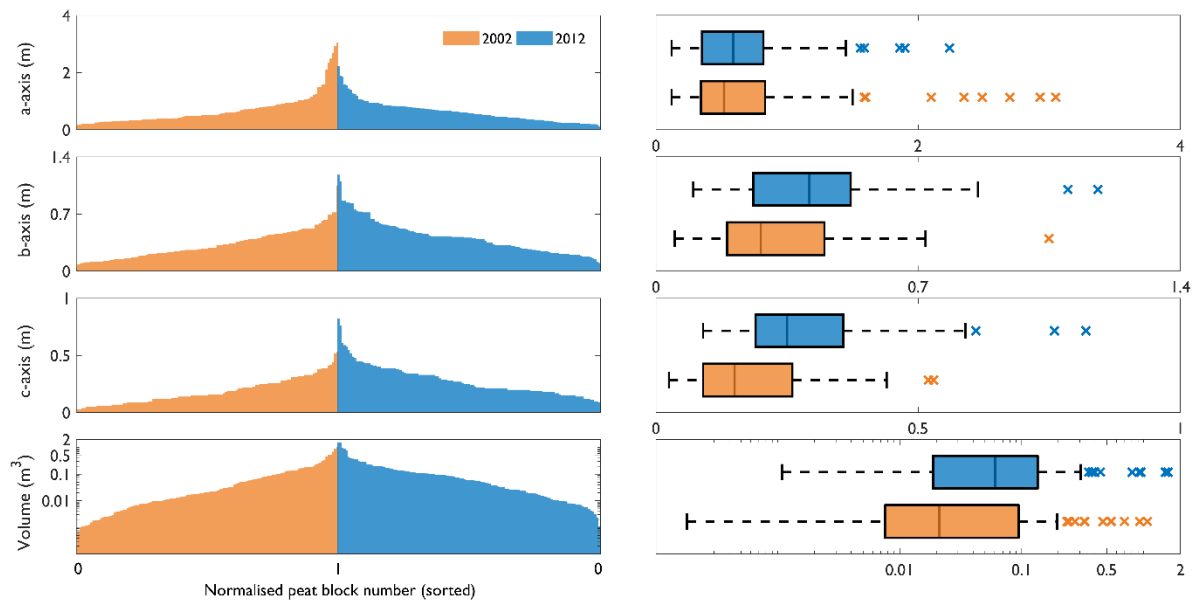


**Figure 5** – Comparison of peat block size (orthogonal axes and volume) between the 2002 and 2012 inventories with peat blocks sorted smallest to largest and normalised by number sampled ( $n = 123$  in 2002;  $n = 127$  in 2012) and same data redrawn as boxplots. Note, same axis scale between plots. Approximately similar distributions are shown between the 2002 and 2012 inventories.

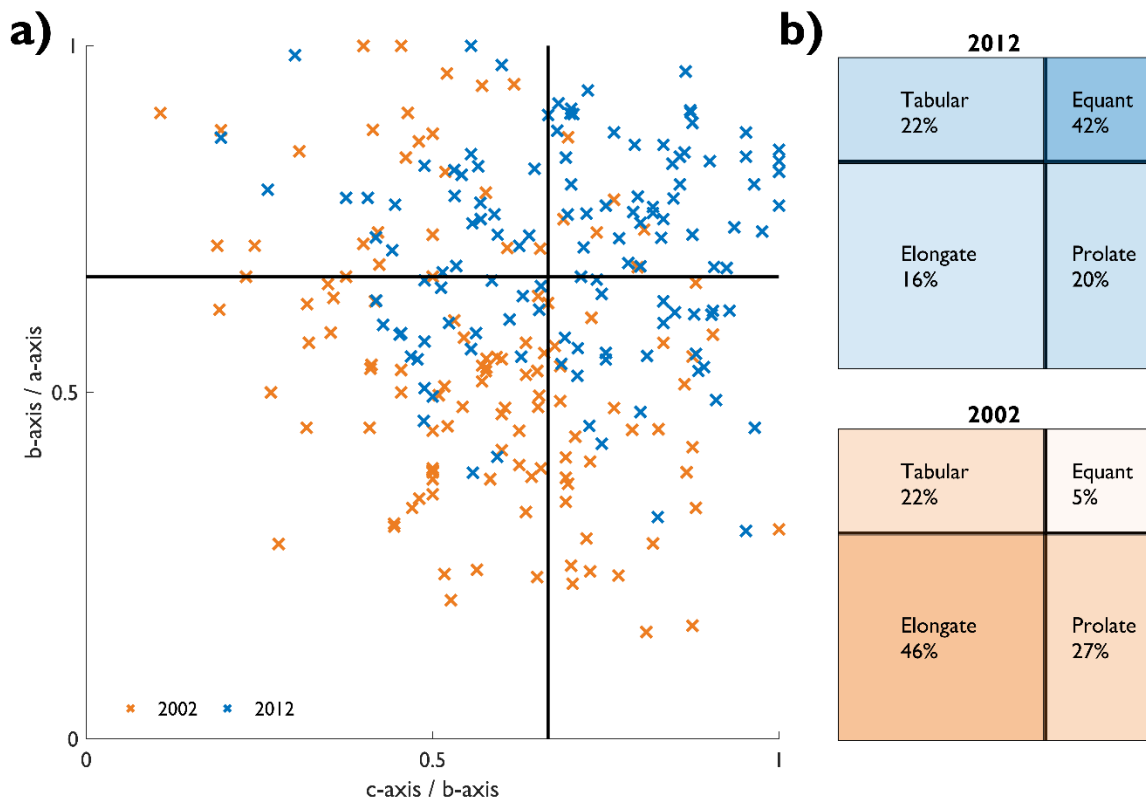


**Figure 6** – Differences in peat block shape between the 2002 and 2012 inventories shown as: (a) Zingg-type diagrams; and (b) as a proportion of peat blocks classified for each block shape (colour intensity scales with the proportion of each peat block shape classified).

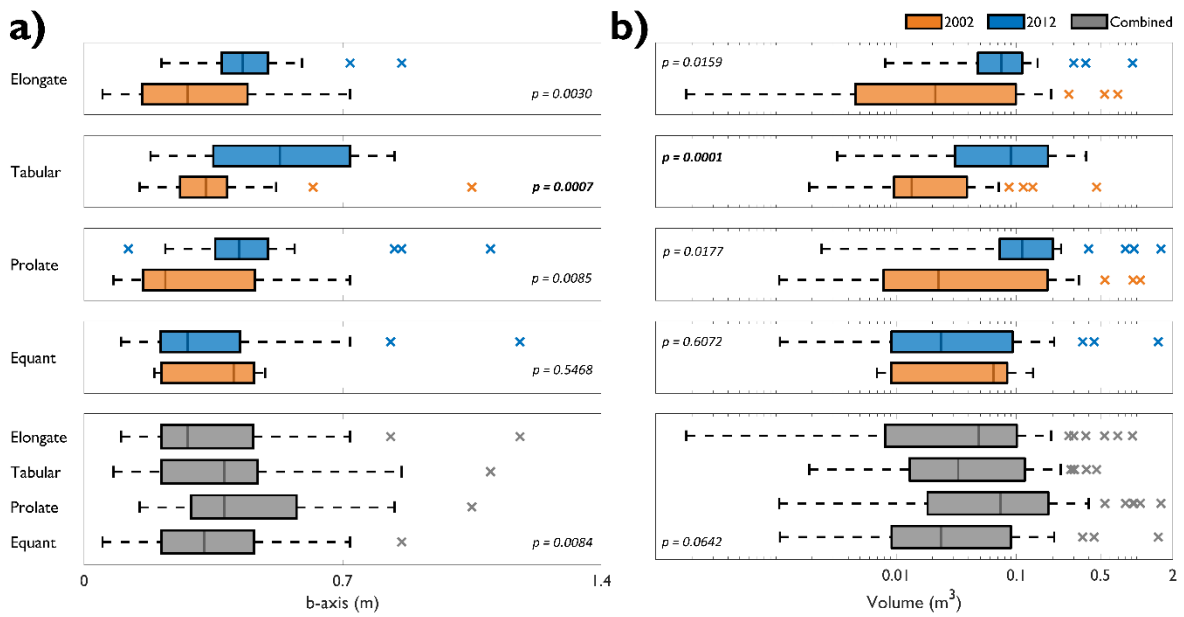


**Figure 7** – Relationship between peat block size and classified shape. Peat block size is defined as: (a) b-axis; and (b) block volume.  $P$ -values show the results of Mann-Whitney tests for size between temporally independent peat block inventories, and Kruskal–Wallis tests between peat blocks of different classified shapes (significance is marked in bold,  $p$ -value < 0.001).

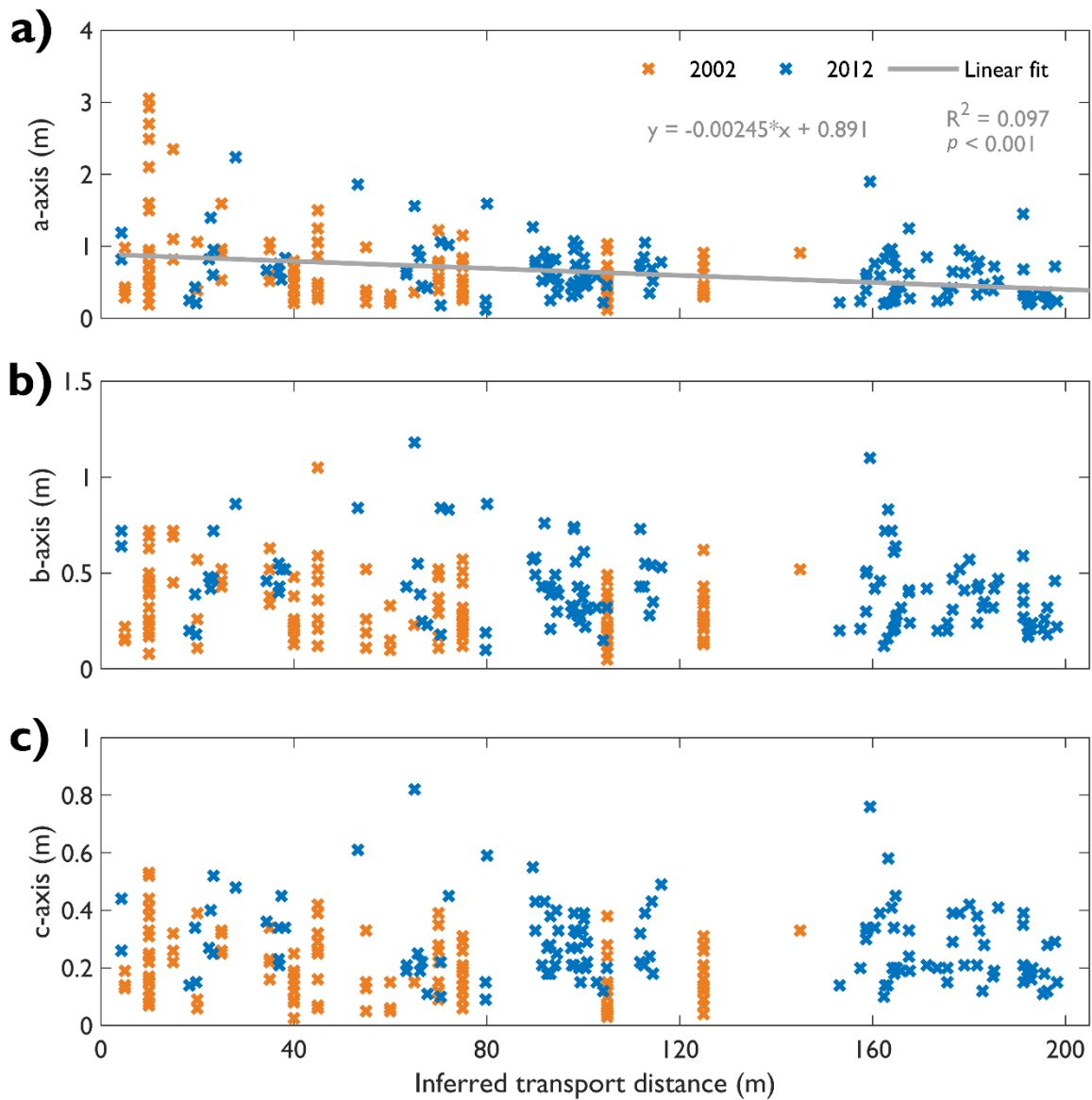


**Figure 8** – Changes in peat block size (a) a-axis, (b) b-axis, (c) c-axis with inferred transport distance for the 2002 and 2012 inventories. The solid grey line represents the linear regression of the 2002 and 2012 combined inventories. Note that a single data point from the 2002 inventory at 345 m is not shown due to visual constraints but is included in the regression.

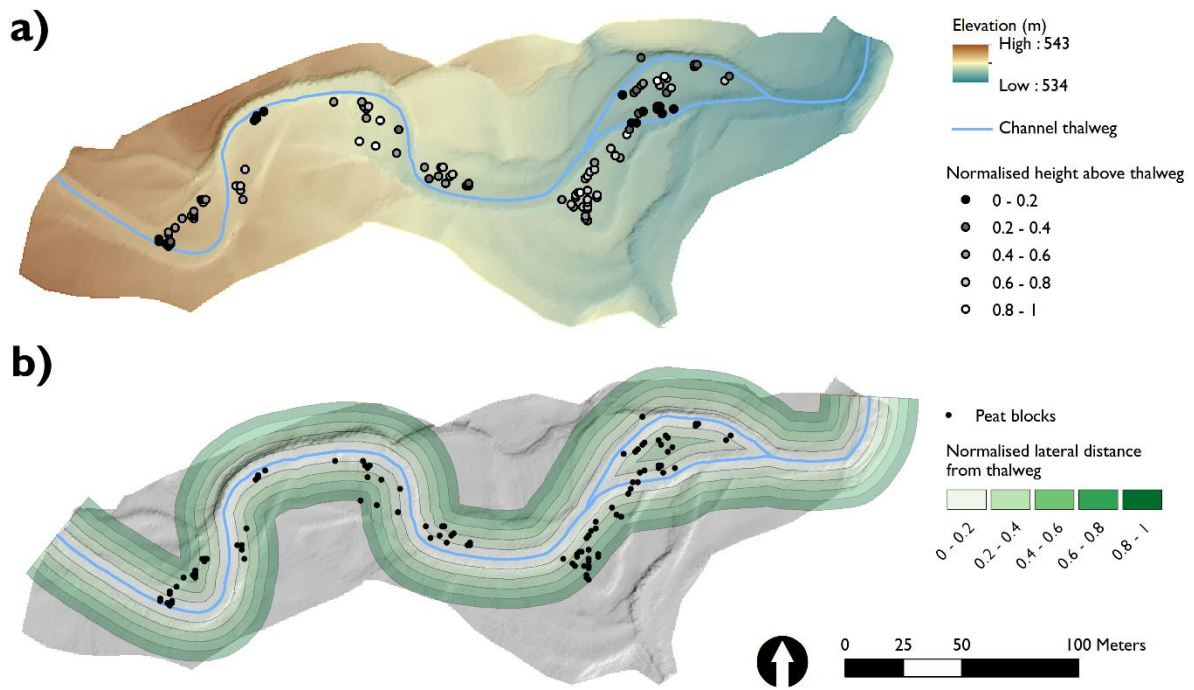


**Figure 9** – Spatial distribution of peat blocks for the 2012 inventory, shown as: (a) normalised height above the channel thalweg; and (b) normalised lateral distance from the channel thalweg. Only peat blocks that were recorded within the DEM coverage area were included for analysis ( $n = 123$ ).

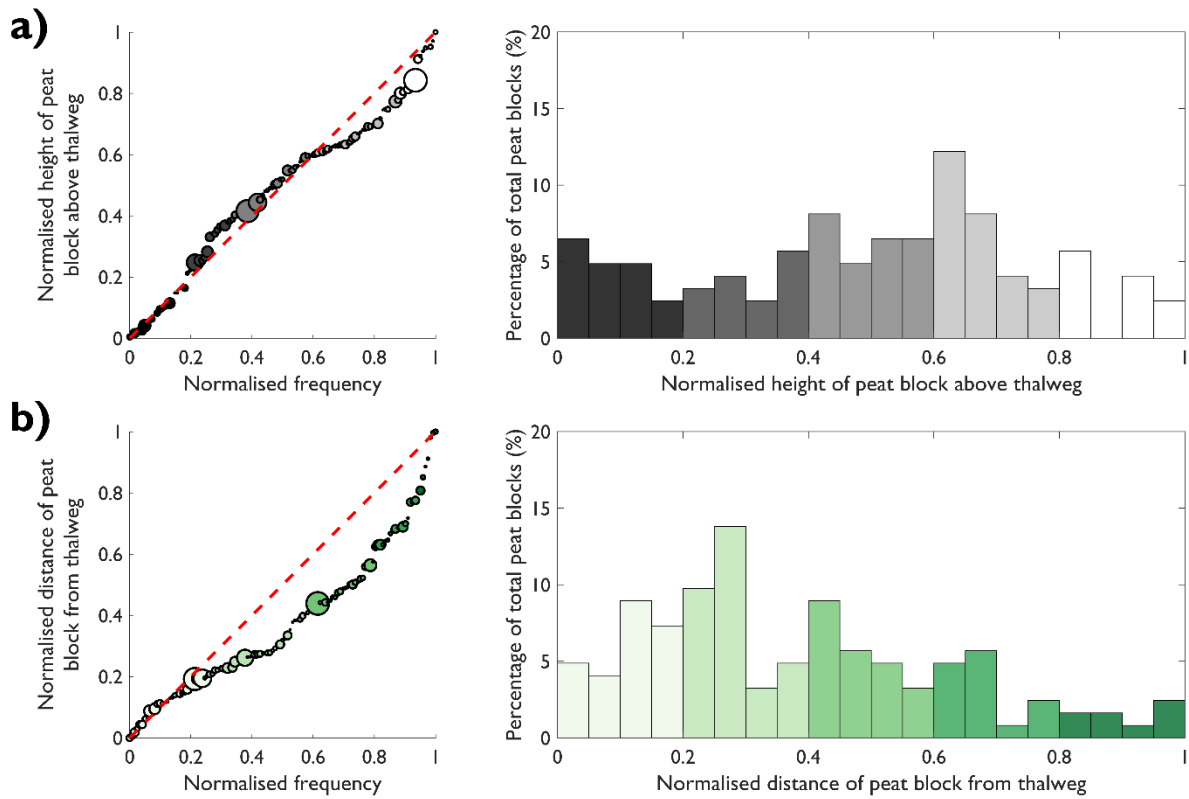


**Figure 10** – Hypsometric relations of peat blocks from the 2012 inventory, shown as: (a) normalised height above the channel thalweg; and (b) normalised distance from the channel thalweg. Colour shading is the same as in Figure 9. Marker points are analytically weighted and proportional in radius to the peat block volume, the line of equality is shown as the red dashed line. Histograms show the percentage of peat blocks at each 0.05 normalised interval.

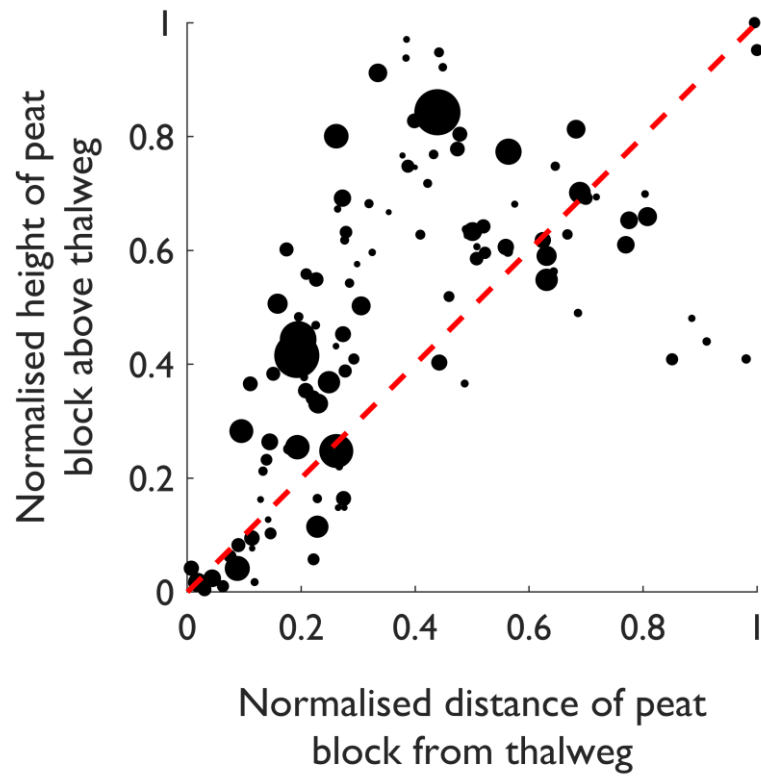


**Figure 11** – Lateral and vertical organisation of mapped peat blocks from the 2012 inventory. Marker points are analytically weighted and proportional in radius to the peat block volume, the line of equality is shown as the red dashed line.